



Accurate Ellipsometric Measurement of Refractive Index and Thickness of Ultrathin Oxide Film

B. M. Ayupov,^a V. A. Gritsenko,^b Hei Wong,^c and C. W. Kim^d

^aNikolaev Institute on Inorganic Chemistry, 630090, Novosibirsk, Russia

^bInstitute of Semiconductor Physics, 630090, Novosibirsk, Russia

^cOptoelectronics Research Center Department of Electronic Engineering, City University of Hong Kong, Kowloon, Hong Kong

^dSamsung Advanced Institute of Technology, Suwon 440-600, Korea

This work presents some suggestions to improve the accuracy of ellipsometry for determining the refractive indices and thicknesses of ultrathin thermal SiO₂ films on silicon. The effects of substrate optical parameter variations on the ellipsometric measurement were ruled out by conducting the ellipsometric measurements in several different media instead of air. An improved ellipsometer adjustment procedure was developed to minimize the error for Ψ and Δ angle measurement and to check the anisotropy of the sample. To extract the thickness and refractive index of ultrathin dielectric film from the light polarization parameters, an optimization technique with fluctuation of substrate parameter taken into account was proposed. Our results show that the refractive indices of ultrathin (2.1–8 nm) thermal oxide films prepared by several different methods fall in the range of 1.475 ± 0.003 .

© 2006 The Electrochemical Society. [DOI: 10.1149/1.2357717] All rights reserved.

Manuscript submitted November 3, 2005; revised manuscript received August 7, 2006. Available electronically October 10, 2006.

The determination of the thickness and the refractive index of ultrathin silicon dioxide (SiO₂) film on Si substrate has become a challenging issue for characterizing the gate oxide growth process of nanoscale metal oxide semiconductor (MOS) devices. Ellipsometry has been considered as an efficient tool for this purpose.^{1,2} In the conventional approach, the refractive index of the ambient was considered as a constant and the thickness and the refractive index of an ultrathin film could be determined from the polarization parameters (Ψ and Δ) of the light reflected from the sample. The accuracy of the measurement is governed by the alignment of the ellipsometric polarizing components, while the accuracy for the parameter calculation is governed by the model of the film being used. With a fixed ambient parameter, the ellipsometric method is able to determine the thickness and the refractive index of an ultrathin oxide film down to about 10 nm.³ Archer³ determined these parameters using the linear relationships for the polarization parameters of the reflected light and the film thickness. The thickness of an ultrathin SiO₂ film on polished Si or Ge wafers was determined from the angle Δ by assuming fixed values of optical parameters for both the oxide film and the substrate. Egorova et al.⁷ improved this method by immersing the sample in different liquids and further extended the accurate measurement down to 2 nm. By measuring the parameters at two different media (liquids with different refractive indices), the substrate optical constants were treated as unknown parameters which were calculated from the data collected from different media.⁵ It was found at $\lambda = 632.8$ nm that the refractive index of dry or wet oxide grown on Si at the temperature of 1150°C remains at a fairly constant level of about 1.467 ± 0.005 for film thicknesses down to 2.0 nm. The immersion method for defining the refractive indices of ultrathin films was also used in the work of one of the authors of this article by assuming that the optical constants of silicon substrate is unknown.⁵ These results agree with Malitson that the thermally grown SiO₂ films have a refractive index close to that of the bulk quartz glass.⁶ Hebert et al.⁷ proposed a single-layer model to determine the refractive index of an ultrathin SiO₂ film.⁷ The film thicknesses was determined with an electrical method.⁸ This method was improved by Wang and Irene with the availability of a multiwavelength (from 250 to 600 nm) light source and a multiple incident angle (from 70 to 75°) ellipsometric data.⁹ In Wang and Irene's work, the refractive index of quartz was used for the initial guess and it was found that the refractive indices of 2.5 and 6.0 nm thick oxide films are 1.9 and 1.7, respectively. These results are significantly larger than those reported by others.^{4,5} We are inclined to believe that values given by Wang and Irene⁹ are overestimated. The discrepancy should be due primarily to the alignment accuracy of the polarized elements in the ellipsometer and the parameter extrac-

tion method for solving the equations. As discussed later in this work, the single-layer model proposed by Hebert et al.⁷ can only be used for films in which refractive index does not vary with the film thickness. For the single-layer model to be used for an ultrathin film, it needs to be improved in several aspects. The idea proposed by one of the present authors can solve these problems.¹⁰

In this work, methods for determining both thickness and refractive index of ultrathin film are presented. The experimental data was obtained either in air or in ambient with different refractive indices. Particular care was taken to ensure the accuracy for the Ψ and Δ angle measurements and the numerical method for determining the film parameters. The present paper is organized as follows. In the next section, we describe the procedures for preparing the SiO₂ films and the optical scheme of the ellipsometer. The results of thickness and refractive index determined using immersion and optimization techniques are presented next, where an improved ellipsometer adjustment procedure is also described in detail. After summarizing the major results of this work, the effects of sample anisotropy, the polarizer and analyzer null angles are formulated in the Appendix.

Experimental

Three types of oxide films were used in this investigation. Conditions for the sample preparation are listed in Table I. Those samples have different thicknesses, ranging from 2.1 to 8 nm, which were measured using the conventional ellipsometric method.³ The wet oxide films (sample set 1) were used to determine the refractive index of the thin SiO₂ films with the immersion method,⁴ whereas the dry oxide films (samples of set 3) were used to determine the optical parameters based on the single-layer film model.^{1,2} For determining the film parameter of N₂O oxide (sample set 2), both single layer and multilayer models were used.

Measurements were carried out on an LEF-3M ellipsometer with a He–Ne laser ($\lambda = 632.8$ nm) light source and a polarizer–compensator–sample–analyzer (PCSA) ellipsometric configuration

Table I. Preparation conditions for thin oxide films used in this investigation.

Sample set	Substrate		Oxidation conditions	
	Orientation	Resistivity (Ω cm)	Method	Temperature range ($^{\circ}$ C)
1	<100> n-Si	4.5	Wet oxide	500–800
2	<100> p-Si	1.5	N ₂ O	700
3	<100> n-Si	7.5	Dry O ₂	700–850

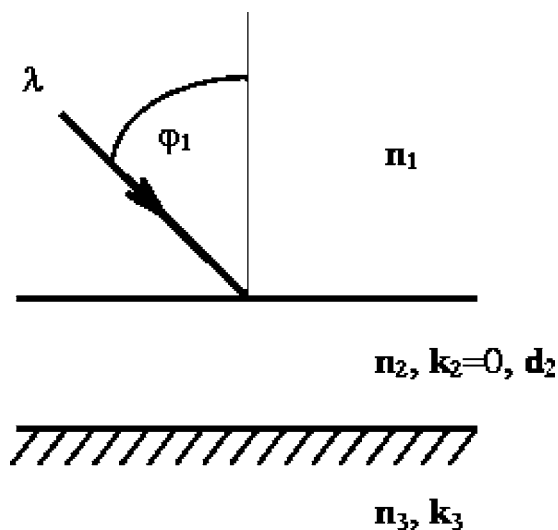


Figure 1. Film structure used in the study: a nonabsorbing single-layer film on an absorbing substrate. φ_1 and λ are the incidence angle and the wavelength of light, respectively.

was used.^{1,2} The light beam first passes through the polarizer (P), compensator (C), and then is incident on the sample (S). The reflection beam from the sample first enters the analyzer (A) and is then detected with a light detector and its reading is registered with a lock-in circuit. The Ψ and Δ angles were obtained with the standard two-zone procedure.^{1,2} The ellipsometric measurements were performed at different incident angles ranging from 50 to 80° with a 5° increment. The inverse problems were solved in succession approximation using a one-, two-, three-, and four-layer model. For the five-layer model calculation, Ψ and Δ angle measurements were performed with two additional incident angles close to the principal incident angle.

Results and Discussion

Immersion experiment.— Consider a system (see Fig. 1) made up by an ambient with medium refractive index n_1 , a nonabsorbing (transparent) film ($k_2 = 0$) with a thickness d_2 , and a refractive index n_2 , and a substrate with a refractive index n_3 and an absorption coefficient k_3 , the relation between the angle Δ and the thickness d_2 for a thin film is linear and is given by Eq. 1 according to the Drude–Archer approximation³

$$\Delta = \Delta_0 - C_\Delta d_2 \quad [1]$$

where Δ_0 is the value of Δ at $d_2 = 0$ and the slope of Δ – d_2 plot C_Δ is given by

$$C_\Delta = \frac{4\pi}{\lambda} n_1 (n_2^2 - n_1^2) \cos \varphi \sin^2 \varphi \left[M \left(\frac{1}{n_2^2} - \alpha \right) + \alpha_1 N \right] \quad [2]$$

The parameters in Eq. 2 are given by

$$M = \cos^2 \varphi - n_1^2 \alpha + n_1^4 (\alpha^2 - \alpha_1^2) \sin^2 \varphi \quad [3]$$

$$N = n_1^2 \alpha_1 - 2n_1^4 \alpha \alpha_1 \sin^2 \varphi \quad [4]$$

$$\alpha = \frac{n_3^2 - k_3^2}{(n_3^2 + k_3^2)^2} \quad [5]$$

$$\alpha_1 = \frac{2n_3 k_3}{(n_3^2 + k_3^2)^2} \quad [6]$$

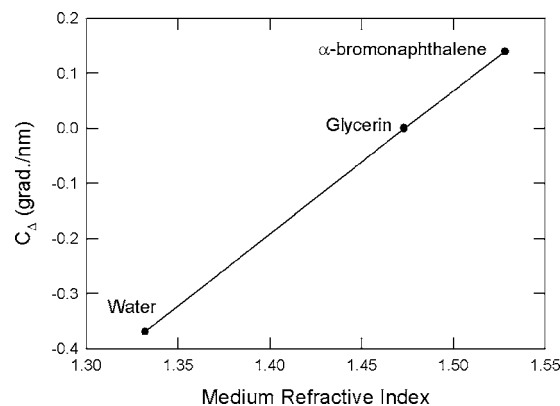


Figure 2. Relation between C_Δ (Eq. 3) and the ambient refractive index for SiO_2 films. The straight line intersects the abscissa at 1.475 ± 0.003 . The refractive index obtained with the single-layer model is 1.473 ± 0.003 .

Note that in Eq. 2, C_Δ is linearly scaled by n_1^2 in general; it is reduced to a linear function of n_1 and approaches to 0 when $n_1 \approx n_2$.

Based on this theory, ellipsometric measurements on some oxide films prepared by wet oxidation method (sample set 1) were conducted. The film thickness was estimated according to the value of angle Δ , in accordance with the Archer method.³ The measurements were performed in air, water, glycerin, and in α -bromonaphthalene. The light incident angle was 40°. The measurements were performed in a flat-bottom plate, where the liquid level was maintained such that the surface of the sample was covered by a 5 mm depth liquid layer.⁵ For each value of the medium refractive index, the magnitude of C_Δ was extracted from the slope of $\Delta - d_2$ plot (see Eq. 1). Figure 2 plots the C_Δ ($\partial\Delta/\partial d_2$) values as a function of the ambient refractive index.

Measurements in liquids yield reliable and precise data. The current measurement procedure for the refractive index does not rely on the information of substrate optical parameter constants. Thus, the variation of substrate optical constants should not cause any difficulties to this method. The possible drawback is that immersion liquids may interact with the object under study. To make sure that the oxide layer does not have any reaction with the immersion liquids, we first measured the angles Ψ and Δ in air and then in immersion liquid and finally in air again to check the possible change after proper cleaning. No notable change was detected.

Improved alignment procedures.— To have a precise measurement of the Ψ and Δ angles, one has to accurately adjust the polarizing elements of the ellipsometer to consider the parameters of the compensator and to ensure that there is no optical anisotropy on the sample. Meanwhile, to guarantee a reliable solution for the inverse problem, sufficient experimental data are indispensable. The accuracy of the ellipsometer adjustment is so important that it had drawn particular attention from several groups.^{7,11} Hebert et al.⁷ adopted the photometric adjustment procedure of Ref. 12. A mercury lamp and metal mirrors were used for the testing.⁷ Initially the compensator was removed from the optical path. At an incident angle close to the principal incident angle, the position of the polarizer was adjusted to locate the minimum light intensity on the analyzer. Then the light incident angle was changed, and the analyzer and polarizer positions were adjusted again to locate the minimum light intensity on the sample. The compensator position was adjusted using the PCA configuration. The anisotropy of the sample, which is particularly important for ultrathin oxide, was not considered in their work. The unrealistic results⁷ obtained from the experiment suggest that the adjustment procedure needs to be improved.

In the present work, we describe, for the first time, the completed procedures for the accurate adjustment in azimuthal scale of the

ellipsometer's polarizing elements based on the preliminary idea reported earlier by one of the authors of this article.¹⁰ In addition, this work also takes the variation of optical parameters and the anisotropy of the silicon surface into account.

To find the correspondence between the positions of the polarizer, compensator, and analyzer optical axes on the azimuthal scales of the components, based on the idea of Ref. 10, we proposed to adjust the apparatus with the following steps:

1. A sample with a smooth surface without any anisotropy was first used. Preliminary ellipsometer adjustment was first attempted. The positions of the polarizer (P_0), analyzer (A_0) and compensator (C_0) were adjusted to align the optical axes of the polarizer and the analyzer. The parameters of the light reflected from the sample at different incident angles (φ), i.e., $\Psi(\varphi)$ and $\Delta(\varphi)$, were used to determine the principal incident angle Φ according to one of the following criteria:¹³ $\Delta = 90^\circ 00'$ or minimum of $\Psi(\varphi)$ which was achieved by performing the measurements in the φ interval of 50° – 80° with a step of 5° decreasing around the Φ value.

2. About 5° difference between the incident angle and the principal angle was set (i.e., $\varphi = \Phi + 5^\circ$). Then the analyzer drum was rotated with a step of $10'$ around the incidence plane (A_p) to find the polarizer and the analyzer setting at extinction vs the analyzer setting. Two linear relationships, $P_1(A_p)$ and $C_1(A_p)$, were obtained.

3. The analyzer was then rotated through the angle $90^\circ 00'$. The analyzer drum was rotated again with a step of $10'$ to find the polarizer and the compensator setting at extinction. Two additional dependences, $P_2(A_s)$ and $C_2(A_s)$, were found. A_s is the position of the analyzer axis near the sample plane.

4. Set the angle of the incident light on the opposite side of the principal incident angle (e.g., $\varphi = \Phi - 5^\circ$). Rotate the analyzer drum with a step of $10'$ to find the third set of linear relationships: $P_3(A_p)$ and $C_3(A_p)$.

5. Rotate the analyzer axis through the angle $90^\circ 00'$ and find the setting at extinction of P and C vs the analyzer position. We obtained fourth set of linear relationships: $P_4(A_s)$ and $C_4(A_s)$.

6. Now place the ellipsometer arms in the straight-through configuration, i.e., the PCA configuration. Rotate the analyzer optical axis to obtain the rectilinear dependences, $P_5(A_p)$ and $C_5(A_p)$.

7. The five pairs of the linear relationships given above can be plotted on graphs with dual analyzer axes (A_p and $A_p + 90^\circ$) and dual polarizer axes (P and $P + 90^\circ$). The compensator axis may be plotted with single axis. If the surface of the sample is isotropic, then the five straight lines $P(A_i)$ ($i = 1, 2 \dots 5$) and the five straight lines $C(A_i)$ will pass through the unique common point for each other.⁵ In the $P(A)$ and $C(A)$ graphs the intersection points are expected to lie at identical values for A and $A + 90^\circ 00'$. These values correspond to A_0 in the preliminary adjustment step.

The presence of optical anisotropy of samples would result in the linear functions, $P(A_i)$ and $C(A_i)$, to have more than one intersection point.⁵ In addition, the graphs can also be plotted in single axis by offsetting the polarizer and the analyzer scales with 90° (see Fig. 3). As shown in Fig. 3, it is seen that the straight lines intersect each other in a narrow interval of analyzer scale. Hence, the proposed adjustment procedure for the polarizing element helps to establish a more accurate correspondence among the polarizer, the analyzer, and the compensator and to their optical axis positions (A_0 , P_0 , C_0) with respect to the incident plane. In addition, it is also able to identify the possible optical anisotropy in the sample. A laser source and a lock-in detector were used to reduce the random errors in determining the setting at extinction¹³ and to establish more accurately the correspondences among the positions of optical components.

Numerical calculation.—Theoretically, even for a single-layer model, there are still five parameters involved: the refractive index and the extinction coefficient of the film (n_2 , k_2), the film thickness (d_2), and the refractive index and the extinction coefficient of the substrate (n_3 , k_3) (Fig. 1). In the method proposed in, Ref. 7 the film

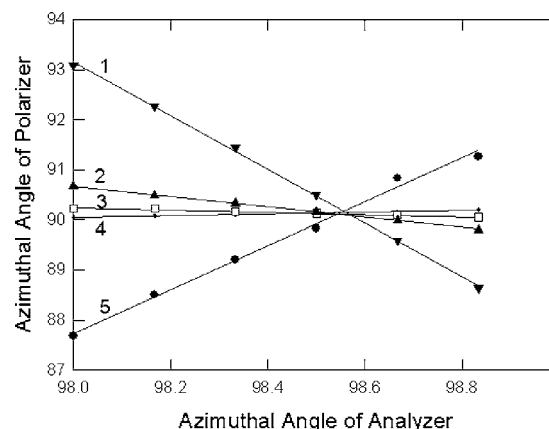


Figure 3. Plot of polarizer angle vs analyzer positions for bare Si substrate during the ellipsometer adjustment process. Line 1: Data obtained when $\varphi = 80^\circ$ and the polarizer axis was positioned near the sample surface. Line 2: Data obtained from PCA configuration. Line 3: $\varphi = 80^\circ$ with analyzer axis being set close to the incident plane. Line 4: $\varphi = 70^\circ$ with analyzer axis being set close to the incident plane. Line 5: when $\varphi = 70^\circ$ with analyzer axis being set close to the sample plane. The polarizer and analyzer scales were reduced by 90° in order to plot the data on the same graph.

thickness was determined with an independent method, and the refractive index was the only parameter to be found as the substrate optical parameters were fixed. However, it seems to be inappropriate to keep the substrate optical parameters as constants. To illustrate the problem, we compare the refractive indices and film thicknesses extracted from different methods. The ellipsometric parameters Ψ and Δ were first measured at various incident angles. Then we calculated the values of n_2 and d_2 for two sets of substrate optical constants. The first set was taken from, Ref. 7 and the other set was obtained in our experiments. Table II lists the values of Ψ and Δ , which were obtained by setting the polarizer and analyzer to extinction. The SiO_2 film was prepared by wet thermal oxidation of Si at 900°C . The procedure used to solve the inverse problem was the same as in Ref. 7, but the final data have a significant difference for all the incident angles in the interval of 50° – 80° . The extracted film thickness spreads from 7.3 to 8.4 nm when the values of Si optical constants reported by Hebert et al.⁷ were used, whereas the use the values reported by Ayupov¹⁰ would result in the film thickness range being reduced to 7.1–8.0 nm. Meanwhile, it is noted that the refractive index has even larger fluctuation ranges. Hebert et al.'s "substrate"⁷ yields a refractive index varying from 2.03 to 2.48, whereas the value of refractive index ranges from 1.90 to 2.31 if the substrate optical constants given by Ref. 10 were used for the calculation. Those values are much larger than the refractive index of bulk quartz glass.

The findings given in Table II suggest that the optical constants of the substrate should not be fixed, and the data measured at dif-

Table II. Calculated thicknesses and refractive indices of oxide films by assuming constant values of the substrate Si parameters.

φ	Ψ	Δ	$N_{\text{Si}} = 3.865 - i0.018^7$		$N_{\text{Si}} = 3.85 - i0.023^{10}$	
			n_2	d_2 (nm)	n_2	d_2 (nm)
50°	$31^\circ 16'$	$174^\circ 32'$	2.37	8.4	2.20	8.0
55°	$27^\circ 16'$	$173^\circ 16'$	2.03	7.2	2.03	7.2
60°	$23^\circ 13'$	$170^\circ 44'$	2.17	7.3	1.90	7.1
65°	$17^\circ 40'$	$166^\circ 05'$	2.22	7.4	1.98	7.1
70°	$10^\circ 51'$	$154^\circ 42'$	2.30	7.5	2.07	7.2
75°	$4^\circ 50'$	$93^\circ 17'$	2.41	7.8	2.22	7.3
80°	$12^\circ 52'$	$20^\circ 20'$	2.48	8.0	2.31	7.5

Table III. Solution to the data listed in Table II obtained by using optimization technique.

Layer	Refractive index	Extinction coefficient	Thickness (nm)
Air	1.00	—	—
Oxide layer	1.46	0.00013	8.6
Si substrate	3.81	0.021	—

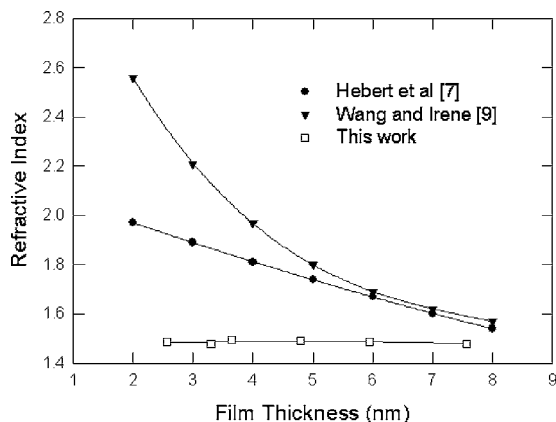
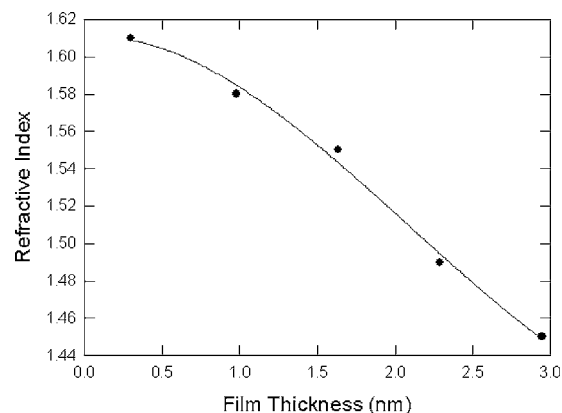
ferent incident angles can be used to minimize the possible error. Here we define an objective function for minimization

$$S = \frac{1}{N} \sum_{i=1}^N \left(\frac{\Psi_{i \text{ exp}} - \Psi_{i \text{ calc}}}{\delta \Psi_{i \text{ exp}}} \right)^2 + \frac{1}{N} \sum_{i=1}^N \left(\frac{\Delta_{i \text{ exp}} - \Delta_{i \text{ calc}}}{\delta \Delta_{i \text{ exp}}} \right)^2 \quad [7]$$

where N is the total number of measurements (at different incident angles), $\Psi_{i \text{ calc}}$ and $\Delta_{i \text{ calc}}$ are the calculated angles Ψ and Δ at the i th incident, and their corresponding experimental values are denoted by $\Psi_{i \text{ exp}}$ and $\Delta_{i \text{ exp}}$, respectively. $\delta \Psi_{i \text{ exp}}$ and $\delta \Delta_{i \text{ exp}}$ are random errors incurred during the measurements. Several methods for minimizing the objective function, S , were reported.¹⁴ Here we use the deformable polyhedron approach.¹⁵ In the deformed polyhedral method, the initial approximations of the sought parameters and their maximum and minimum values are specified. For the optical model with m parameters, $(m + 1)$ points of parameters were constructed. These points are equidistant from each other in the m -dimensional space. The goal functions S serve as the tops of the m -dimensional simplex. When the parameters of the model changes, operations such as reflection, expansion, compression, and reduction, will be performed to finding the simplex's top with the minimal objective function. When next step's changes are less than some given number, the minimal objective function is considered to be achieved.

Minimizing the objective function in Eq. 7, the solution to the data given in Table II is listed in Table III. The mean difference between the calculated and experimental Ψ and Δ values is only $6'$, and the refractive index of the film obtained with this method is equal to that of quartz glass¹⁶ and seems to be more reasonable.

Figure 4 compares the data reported by others^{7,9} (solid markers) and the data calculated with the objective function minimization technique (open markers) as given above. As shown in Fig. 4, the refractive index of the SiO_2 film reported by Hebert et al.⁷ and Wang and Irene⁹ can be significantly larger than that of a quartz silica and shows a strong thickness dependency. An exponential dependence of refractive index on the film thickness was found. The refractive index at the Si– SiO_2 interface is 3.85; it reduces to 2.4 and 1.7 for 2.5 and 6.0 nm thick films, respectively. The averaged value for the

**Figure 4.** Refractive indexes of SiO_2 films obtained based on a single-layer model.**Figure 5.** Plot of refractive index as a function of film thickness. The oxide films were grown by oxidizing the silicon substrates in N_2O ambient at 700°C .

film thickness in this range is about 1.894 ± 0.110 . This is a questionable outcome as it is commonly accepted that the single-layer model is only applicable to the cases in which the refractive index does not depend on the film thickness.^{1,2} The refractive index calculated with the present method (open markers) falls in the range of 1.48–1.49 and weakly depends on the film thickness. The findings seem to be more reasonable.¹⁷

The present method was also extended to multilayer model cases. Figure 5 shows the results for N_2O oxide grown on Si (sample set 2). Nine pairs of Ψ and Δ values were collected. The refractive index is found to increase as the oxide layer becomes thinner. The mean difference between the calculated and experimental values of Ψ and Δ is $5'$. It was shown in Ref. 18 that N_2O oxides were predominantly silicon dioxide. The refractive indices (first two open markers in Fig. 4) falling in the range of 1.48–1.49 is a good confirmation. For thermal oxidation the refractive indexes of the films vary within 1.46–1.49. These figures agree with the findings obtained in the immersion experiment.

Factors affecting the measurement accuracy.—The accuracy in the determination of reflected-light polarization parameters is affected by: (i) optical anisotropy of the sample, (ii) compensator parameters, and (iii) position of the compensator axis.

The mechanically polished silicon substrates may be anisotropic.¹⁰ This anisotropy can be described by the coefficients of the reduced Jones matrix.^{1,2} Our calculations, using the formula given in Ref. 12 show that Ψ_{sp} is in the range of $0^\circ 30'$ to $1^\circ 00'$ for a uniaxial crystal with $n_o = 3.85$, $n_e = 3.90$, $k_o = 0.023$, and $k_e = 0.030$ at the light incident angle of 70° , inclination angle of the optical axis of 10° , and rotation angles of 77 and 105° .

Considering these factors, a virtual sample with $\Psi = 10^\circ 15'$ and $\Delta = 172^\circ 00'$ was constructed using the formulas given in the Appendix, where formulas for proper corrections of the compensator parameters are also given. We calculated the Ψ and Δ angles by varying the nondiagonal elements of the reflection matrix with 1° step, and by varying the compensator parameters and compensator axis setting. It was found that a predominant contribution to the change of Ψ and Δ angles is from the optical axis setting of the compensator. Thus, the ellispometer adjustment is of vital importance for the precision measurement. Table IV lists the Ψ and Δ values from two-zone measurements for both isotropic and anisotropic samples. It can be seen from Table IV that if the compensator axis is miss-positioned for a degree, a 2° change in the measured parameter Δ and $30'$ change in Ψ will result; in other words, the adjustment accuracy of the azimuthal axes of the polarizing components is a decisive factor in governing the accuracy of the reflected light polarization parameters.

Table IV. Effects of sample parameters, compensator parameters, and compensator azimuthal angles variations on the reflected light polarization parameters.

Ψ_{sp}	Ψ_c	Δ_c	C	Ψ_{34}	Δ_{34}
0°00'	45°00'	90°00'	-45°00'	10°15'	172°00'
0°30'	45°00'	90°00'	-45°00'	10°15'	172°00'
1°00'	45°00'	90°00'	-45°00'	10°15'	172°00'
0°00'	44°30'	90°00'	-45°00'	10°15'	172°00'
0°00'	44°00'	90°00'	-45°00'	10°15'	172°00'
0°00'	45°00'	89°30'	-45°00'	10°15'	172°00'
0°00'	45°00'	89°00'	-45°00'	10°15'	172°00'
0°00'	45°00'	90°00'	-44°30'	10°15'	171°00'
0°00'	45°00'	90°00'	-44°00'	9°46'	170°00'
0°00'	45°00'	90°00'	-46°00'	10°46'	174°00'

Meanwhile, the range of Ψ values for nonabsorbing films on Si ($n_3 = 3.85$ and $k_3 = 0.023$) at $\varphi = 70^\circ$ and $\lambda = 632.8$ nm is rather narrow. For instance, a film with 1.3 nm thick and refractive index of 2.5 would produce parameter values $\Psi = 10^\circ 43'$ and $\Delta = 175^\circ 00'$; for sample with 2.2 nm thick and with refractive index of 1.40, the corresponding polarizing parameters are $\Psi = 10^\circ 47'$ and $\Delta = 171^\circ 43'$. It is further noted that the system error for Ψ at $C = -44^\circ 00'$ or $C = -46^\circ 00'$ is much larger than the Ψ data range for ultrathin films. It is illustrated again that the accuracy ellipsometer adjustment is crucial for the ultrathin film measurements.

Conclusions

This work introduces several suggestions to improve the accuracy of ellipsometry for determining the thickness and refractive index of ultrathin dielectric film on silicon. The effects of misalignment of the polarizing component, substrate optical parameter fluctuation, and the sample anisotropy were characterized and discussed. A rigorous adjustment procedure of the polarizing components was proposed, and an objective function was constructed for determining the film parameters using the optimization technique. The refractive indices of ultrathin (2.1–8 nm) thermal oxide films prepared by several different methods are in the range of 1.475 ± 0.003 . This is a great improvement compared with some previous reports, for example, Wang and Irene's work.⁹ Wang and Irene found that the refractive indices of 2.5 and 6.0 nm thick oxide films are 1.9 and 1.7, respectively.⁹ These values are not consistent with the commonly accepted value of the refractive index of SiO₂ (about 1.4) which was obviously overestimated.

Acknowledgments

The work described in this paper was supported by the Siberian Branch of the Russian Academy of Sciences and Ministry of Industry (project no. 116), Ministry of Technologies and Science of the Russian Federation (grant no. NSh--1042.2003.3 and 02.435.11.2012), a UGC Competitive Earmarked Research Grant of Hong Kong (project no. CityU 1167/03E), and National Program for Tera-Level Nanodevice of the Korea Ministry of Science and Technology.

Appendix

In this Appendix, formulas for calculating the polarizer and analyzer setting at extinction for an arbitrary position of the compensator optical axis are derived. Anisotropic sample was assumed for the derivation. The relationship between the light incident and reflection for an anisotropic sample is given by^{1,2}

$$\begin{pmatrix} E_p^{(1)} \\ E_s^{(1)} \end{pmatrix} = \begin{pmatrix} r_{pp} r_{ps} \\ r_{sp} r_{ss} \end{pmatrix} \begin{pmatrix} E_p^{(0)} \\ E_s^{(0)} \end{pmatrix} \quad [\text{A-1}]$$

or

$$\frac{E_p^{(1)}}{E_s^{(1)}} = \frac{r_{pp} E_p^{(0)} + r_{ps} E_s^{(0)}}{r_{sp} E_p^{(0)} + r_{ss} E_s^{(0)}} \quad [\text{A-2}]$$

where r_{ps} and r_{sp} are the nondiagonal elements of the reflection matrix.

Defining $\rho_1 = E_p^{(1)}/E_s^{(1)}$, $\rho_0 = E_p^{(0)}/E_s^{(0)}$, $R_{pp} = r_{pp}/r_{ss}$, $R_{ps} = r_{ps}/r_{ss}$, and $R_{sp} = r_{sp}/r_{ss}$, Eq. A-2 reduces to

$$\rho_1 = \frac{R_{pp}\rho_0 + R_{ps}}{1 + R_{sp}\rho_0} \quad [\text{A-3}]$$

and

$$\rho_0 = \frac{R_{ps} - 1}{\rho_1 R_{sp} - R_{pp}} \quad [\text{A-4}]$$

For PCSA ellipsometric configuration, the polarization of the light passing through the polarizer and compensator, i.e., the polarization of the beam incident on the sample, is given by¹⁹

$$\rho_0 = \frac{\tan C + \rho_c \tan(P - C)}{\rho_c \tan C \tan(P - C) - 1} \quad [\text{A-5}]$$

where ρ_c is the compensator parameter, and C and P are azimuthal angles of the compensator and polarizer, respectively.

Equating A-4 and A-5, we have

$$\frac{\tan C + \rho_c \tan(P - C)}{\rho_c \tan C \tan(P - C) - 1} = \frac{R_{ps} - 1}{\rho_1 R_{sp} - R_{pp}} \quad [\text{A-6}]$$

At the extinction (at minimum detector light intensity), the analyzer azimuthal angle and the polarization of the light reflected from the sample are related by¹⁹

$$\rho_1 = \cot A \quad [\text{A-7}]$$

By substituting Eq. A-7 into A-6, one can see that the values of the polarizer and analyzer setting at extinction at a fixed value of the compensator azimuthal angle are determined by the reflection-matrix elements. Equation A-6 contains complex value parameters, i.e., $R_{ps} = R'_{ps} + iR''_{ps}$. This equation can be split into a real part and an imaginary part and yields a system of two nonlinear equations with two unknowns. This system was solved as the function of the analyzer.²⁰ It can also be solved as the function of the compensator for calculation of parameters Ψ and Δ

$$\tan A = \frac{a_1 b_2 - a_2 b_1 + a_4 b_3 - a_3 b_4 \mp X}{2(a_1 b_3 - a_3 b_1)} \quad [\text{A-8}]$$

$$\tan(P - C) = \frac{a_2 b_1 - a_1 b_2 + a_4 b_3 - a_3 b_4 \pm X}{2(a_2 b_3 - a_3 b_2)} \quad [\text{A-9}]$$

where

$$X = \sqrt{(a_1 b_2 - a_2 b_1 + a_3 b_4 - a_4 b_3)^2 - 4(a_4 b_1 - a_1 b_4)(a_2 b_3 - a_3 b_2)} \quad [\text{A-10}]$$

$$a_1 = R'_{ps} - R''_{pp} \tan C$$

$$b_1 = R''_{ps} - R''_{pp} \tan C$$

$$a_2 = \rho_c'(R'_{sp} + \tan C) - \rho_c''R''_{sp}$$

$$b_2 = \rho_c'R''_{sp} + \rho_c''R'_{sp}$$

$$a_3 = \rho_c'(R'_{ps} \tan C + R''_{pp}) - \rho_c''(R''_{ps} \tan C + R''_{pp})$$

$$b_3 = \rho_c'(R''_{ps} \tan C + R''_{pp}) + \rho_c''(R'_{ps} \tan C + R''_{pp})$$

$$a_4 = 1 - R'_{sp} \tan C$$

$$b_4 = -R''_{sp} \tan C$$

As can be seen from Eq. A-8 and A-9, each value of the compensator azimuthal angle corresponds to two values of polarizer and analyzer azimuthal angles.

References

1. A. V. Rzanov, K. K. Svitashov, A. I. Semenenko, L. V. Semenenko, and V. K. Sokolov, *Principles of Ellipsometry*, Nauka, Novosibirsk (1970).
2. R. M. A. Azzam and N. M. Bashara, *Ellipsometry and Polarized Light*, North-Holland, Amsterdam (1997).
3. R. J. Archer, *J. Electrochem. Soc.*, **104**, 619 (1957).
4. G. A. Egorova, N. S. Ivanova, E. V. Patapov, and A. V. Rakov, *Optika Spektroskopija*, **36**, 773 (1974).
5. B. M. Ayupov and N. P. Sysoeva, *Cryst. Res. Technol.*, **11**, 503 (1981).
6. J. N. Malitson, *J. Opt. Soc. Am.*, **55**, 1205 (1965).
7. K. J. Hebert, S. Zafar, E. A. Irene, R. Kuehn, T. E. McCathy, and E. K. Demirlioglu, *Appl. Phys. Lett.*, **68**, 266 (1996).
8. S. Zafar, K. A. Conrad, Q. Liu, E. A. Irene, G. Hames, R. Kuehn, and J. J. Wortman, *Appl. Phys. Lett.*, **67**, 1031 (1995).
9. Y. Wang and E. A. Irene, *J. Vac. Sci. Technol. B*, **18**, 279 (2000).
10. B. M. Ayupov, *Optik (Jena)*, **109**, 145 (1998).
11. V. N. Fedorinin and V. K. Sokolov, *Optika Spektroskopija*, **70**, 1169 (1991).
12. F. L. MacCrackin, E. Passaglia, R. R. Stromberg, and H. L. Steinberg, *J. Res. Natl. Bur. Stand., Sect. A*, **67A**, 363 (1963).
13. G. Junck, *Philos. Mag.*, **70**, 493 (1994).

14. T. E. Shoup, *A Practical Guide to Computer Methods to Engineers*, Prentice-Hall, New York (1979).
15. J. A. Nelder and R. Mead, *Comput. J.*, **7**, 308 (1964).
16. F. I. Fedorov and V. V. Filippov, *Reflection and Refraction of Light by Transparent Crystal*, Nauka I Technika, Minsk (1976).
17. V. A. Zolotarev, E. V. Morozov, and E. V. Smirnova, *Optical Constants of Natural and Technical Mediums*, Chemistry, Leningrad (1984).
18. V. A. Gritsenko, H. Wong, W. M. Kwok, and J. B. Xu, *J. Vac. Sci. Technol. B*, **21**, 241 (2003).
19. R. M. A. Azzam and N. M. Bashara, *J. Opt. Soc. Am.*, **62**, 222 (1972).
20. B. M. Ayupov and S. A. Prokhorova, *Opt. Spectrosc.*, **90**, 446 (2001).